Impaired In Vivo Mitochondrial Krebs Cycle Activity After Myocardial Infarction Assessed Using Hyperpolarized Magnetic Resonance Spectroscopy

Michael S. Dodd, DPhil[#], **Helen J. Atherton, PhD**[#], **Carolyn A. Carr, DPhil**, **Daniel J. Stuckey, DPhil**, **James A. West, PhD**, **Julian L. Griffin, DPhil**, **George K. Radda, DPhil**, **Kieran Clarke, PhD**, **Lisa C. Heather, DPhil**, and **Damian J. Tyler, PhD**
Department of Physiology, Anatomy, and Genetics, University of Oxford, Oxford, United Kingdom (M.S.D., H.J.A., C.A.C., G.K.R., K.C., L.C.H., D.J.T.); Centre for Advanced Biomedical Imaging, University College London, London, United Kingdom (D.J.S.); and Department of Biochemistry, University of Cambridge, Cambridge, United Kingdom (J.A.W., J.L.G.)

[#] These authors contributed equally to this work.

Abstract

Background—Myocardial infarction (MI) is one of the leading causes of heart failure. An increasing body of evidence links alterations in cardiac metabolism and mitochondrial function with the progression of heart disease. The aim of this work was to, therefore, follow the in vivo mitochondrial metabolic alterations caused by MI, thereby allowing a greater understanding of the interplay between metabolic and functional abnormalities.

Methods and Results—Using hyperpolarized carbon-13 (^{13}C)-magnetic resonance spectroscopy, in vivo alterations in mitochondrial metabolism were assessed for 22 weeks after surgically induced MI with reperfusion in female Wister rats. One week after MI, there were no detectable alterations in in vivo cardiac mitochondrial metabolism over the range of ejection fractions observed (from 28% to 84%). At 6 weeks after MI, in vivo mitochondrial Krebs cycle activity was impaired, with decreased ^{13}C-label flux into citrate, glutamate, and acetylcarnitine, which correlated with the degree of cardiac dysfunction. These changes were independent of alterations in pyruvate dehydrogenase flux. By 22 weeks, alterations were also seen in pyruvate dehydrogenase flux, which decreased at lower ejection fractions. These results were confirmed using in vitro analysis of enzyme activities and metabolomic profiles of key intermediates.

Conclusions—The in vivo decrease in Krebs cycle activity in the 6-week post-MI heart may represent an early maladaptive phase in the metabolic alterations after MI in which reductions in Krebs cycle activity precede a reduction in pyruvate dehydrogenase flux. Changes in mitochondrial metabolism in heart disease are progressive and proportional to the degree of cardiac impairment.

Keywords

citric acid cycle; heart; magnetic resonance spectroscopy; metabolism; myocardial infarction

Myocardial infarction (MI) is the leading cause of heart failure in the developed world and results in high levels of mortality and morbidity in patients.[1] MI is caused by a partial or complete obstruction of a coronary artery, resulting in significant reductions in coronary blood flow and in ischemia.[2] MI injury results in loss of heart tissue, causing the heart to remodel structurally and metabolically. However, this remodeled state is unsustainable, and the heart eventually fails, where the myocardial wall thins, the left ventricular (LV) cavity dilates, and cardiac output decreases.[2] After a MI, the progression into heart failure can be characterized by profound changes in myocardial energy metabolism.[1,3]

Fatty acid oxidation contributes 60% to 70% of the energy required for the resting heart, with glucose and lactate making up the majority of the remaining needs.[1,2,4,5] The tightly regulated reciprocal relationship between glucose oxidation through pyruvate dehydrogenase (PDH) and fatty acid oxidation breaks down after an MI.[5–7] This is accompanied by alterations in both Krebs cycle enzyme activities and electron chain complexes and contributes to a generalized reduction in the capacity for ATP production.[8–12] In vitro experiments of MI have revealed that there are alterations in the electron transport chain as early as 2 weeks after MI,[8] and that alterations in cardiac mitochondrial metabolism continue out to 6 months. However, the exact nature and timing of in vivo mitochondrial dysfunction after an MI are unclear, and information about this would provide a greater understanding of the development of metabolic abnormalities after an MI.

The use of hyperpolarized ^{13}C-magnetic resonance spectroscopy (MRS)[13] allows the study of in vivo mitochondrial metabolism by measuring the flux of ^{13}C-labeled pyruvate through PDH and into the Krebs cycle.[14–18] Unlike positron emission tomography, which uses substrates such as ^{18}Fluorodeoxyglucose as a marker of glucose uptake, or in vitro enzyme assays, hyperpolarized ^{13}C-MRS provides a noninvasive, in vivo real-time measurement of metabolic flux.[13,15,19–21] The technique allows animals to be scanned serially, thereby offering the potential to track the temporal metabolic changes associated with MI and heart failure progression in vivo.

The aims of this study were to assess in vivo metabolic alterations in mitochondrial function that occur after an MI. Rats were scanned using both hyperpolarized [1-^{13}C] and [2-^{13}C] pyruvate at 1, 6, and 22 weeks after MI. Cardiac function was monitored at each time point using echocardiography. Ejection fraction (EF) was used to correlate in vivo metabolic data with the severity of cardiac functional impairment. Ex vivo metabolomics and biochemical

analysis of enzyme activities were used to support the in vivo data at the 22-week time point.

Methods

Detailed Methods are presented in the Data Supplement. Fifteen female Wistar rats (200–250 g; 8–9 weeks; Harlan, United Kingdom) were housed on a 12:12-hour light/dark cycle in animal facilities at the University of Oxford. All animal studies were performed between 7 am and 1 pm with the animals in the fed state. All investigations conformed to Home Office Guidance on the Operations of the Animals (Scientific Procedures) Act 1986, to institutional guidelines and were approved by the University of Oxford Animal Ethics Review Committee.

MI Surgery

Surgical procedures were performed to ligate the left anterior descending coronary artery as previously described.[22] Eleven anaesthetized female Wistar rats underwent 50 minutes of ischemia followed by reperfusion (2%–3% isoflurane in oxygen). Four sham-operated animals underwent the same procedure but without ligation of the left anterior descending.

Echocardiography

Animals were lightly anaesthetized with isoflurane (1.5% in 2 L/min oxygen) and 2-dimensional-echocardiography was performed as described.[22] Measurements of end-diastolic and end-systolic areas and diameter were used to determine EFs (end-diastolic area – end-systolic area/end-diastolic area) at 1, 6, and 22 weeks after MI.[22]

MRI Measurements of Cardiac Function

At 22 weeks after MI, cardiac structure and function were also assessed using CINE MRI as previously described.[20] Briefly, anaesthetized animals (1.5%–2% isoflurane in 2 L/min oxygen) were positioned in an 11.7 T vertical bore MR scanner (Magnex Scientific, Oxon, United Kingdom) interfaced to a Bruker Avance console (Bruker Medical, Ettlingen, Germany) and a shielded gradient system (Magnex Scientific). A 52-mm birdcage transmit/receive radiofrequency coil was used to obtain MRI (Rapid Biomedical, Rimpar, Germany). Sequences were ECG-triggered, and 24 to 31 frames were collected per cardiac cycle. For each heart, the LV mass, EF, stroke volume, scar size, and cardiac output were derived using the free-hand drawing function in ImageJ (National Institutes of Health). The infarct size was determined by measuring the akinetic region in the image.[22]

Hyperpolarized 13C-MRS Protocol

At 1, 6, and 22 weeks after MI, animals were scanned with both [1-^{13}C]pyruvate and [2-^{13}C]pyruvate (Sigma-Aldrich, Gillingham, United Kingdom), as previously described.[15,23] Briefly, anaesthetized animals (1.5%–2% isoflurane in 2 L/min oxygen) were positioned in a 7T horizontal bore MR scanner (Varian Inc, Yarnton, United Kingdom), and signal from the heart was localized using a custom-built ^{1}H/^{13}C butterfly coil. Correct positioning was confirmed with an axial proton fast low-angle shot image, and an ECG-gated shim was used to reduce the proton line width to ≈120 Hz. One milliliter of either

hyperpolarized [1-^{13}C]- or [2-^{13}C]pyruvate was injected >10 s through a tail vein cannula (dose of 0.32 mmol/kg). Sixty individual, ECG-gated, ^{13}C-MR pulse-acquire cardiac spectra were acquired after injection (TR, 1 s; excitation flip angle, 5°; sweep width, 13 593 Hz; acquired points, 2048; frequency centered on the C1 pyruvate resonance, total acquisition time, 60 s). The [1-^{13}C]pyruvate and [2-^{13}C]pyruvate infusions were conducted ≈1 hour apart in all animals, and the sequence of infusions was randomized.

MRS Data Analysis

Cardiac 13C-MRS spectra were analyzed as previously reported.[20] Briefly, for [1-^{13}C]pyruvate MRS data, the peak areas of metabolites at each time point were quantified using a kinetic model.[16] The acquired [2-^{13}C]pyruvate spectra were summed for the first 30 s after the appearance of [2-^{13}C]pyruvate, to increase the sensitivity of measurements because of a low signal:noise ratio. The peak areas of metabolites were quantified in the summed spectra.

Tissue Collection

One day after the 22-week hyperpolarized scans, animals were anaesthetized using an overdose of isoflurane. The hearts were removed and placed in ice-cold PBS (Sigma-Aldrich). The hearts were immediately blotted, the scar excised and viable tissue weighed before being freeze–clamped, and stored at −80°C for subsequent biochemical analysis.

Tissue Homogenization and Enzyme Activity Assays

Tissue was homogenized using the following method for all assays unless stated otherwise. Frozen powered cardiac tissue (15 mg) was homogenized in 1 mL of ice-cold homogenization buffer using a polytron homogenizer (Kinematic, Luzern, Switzerland) for 30 s. To each sample, 10 μL of triton X-100 was added before being briefly vortexed and incubated on ice for 10 minutes. Samples were centrifuged (375g for 10 minutes at 4°C), and used for assays as described below.

The activity of citrate synthase (CS) was determined spectrophotometrically in a reaction that monitored the increase in absorbance at 412 nm because of the conversion of 5,5′-dithiobis(2-nitrobenzoic acid) to 2-nitro-5-thiobenzoate.[5] The activity of carnitine acetyl-transferase was determined spectrophotometrically in a coupled reaction monitoring the production of nicotinamide adenine dinucleotide using previously developed methods.[24] The activity of isocitrate dehydrogenase and aconitase was determined spectrophotometrically.[25] The activity of PDH was measured using a spectrophotometric assay, as previously described.[20] The cardiac tissue used for the PDH activity assay was homogenized in different buffers depending on whether the active or total activity was analyzed. The reaction monitored the increase in absorbance at 340 nm because of the reduction of nicotinamide adenine dinucleotide to nicotinamide adenine dinucleotide, in the active and maximally active (total) PDH fractions. PDH activity was expressed as a percentage of the ratio of active to total.

NMR Metabolomic Analysis

Metabolites were extracted using methanol–chloroform–water, and the aqueous extract was analyzed as previously described using both gas chromatography-mass spectrometry and ^{1}H-NMR spectroscopy.[26] The following metabolites were assessed: glutamate, citrate, malate, and creatine. Data were expressed as relative to the control peak of TSP.

Acylcarnitine-Free Carnitine Assay

Cardiac tissue (50 mg) was pulverized and extracted using methanol/chloroform/water. Butylated extracts were injected (10 μL) into a Quattro Premiere XE Triple Quadrupolar Mass Spectrometer (Waters Ltd, Elstree, United Kingdom) coupled with an electrospray ionization source in positive ion mode. The acylcarnitines were analyzed by multiple reaction monitoring in a positive ion mode. Samples were introduced by direct infusion. Data were processed using the Neolynx software package (Waters Ltd).

Statistics

All data underwent a Kolmogorov–Smirnov normality test with the Dallal–Wilkinson–Lillie for corrected *P* value. All results were expressed as correlations against the assessed EF, across the shams and infarcted animals. Data that were normally distributed underwent a Pearson linear regression test; all others underwent a Spearman Rank. Statistical significance was defined as $P \leq 0.05$. In addition, a group analysis (Data Supplement) was undertaken to compare the hearts with an EF>65% (normal function n=6) with those with an EF<50% (impaired function n=5). A 2-tailed Student *t* test was performed to assess statistical differences between the groups in the group analysis. All statistical analysis was undertaken using Prism 6 (GraphPad Software, San Diego, CA). All graphs show a trendline of linear regression with the 95% confidence levels indicated by the displayed bounds.

Results

Alterations in Cardiac Structure and Function After Myocardial Function

Echocardiography showed that 1 week after surgery, animals that had undergone MI surgery displayed a range of EFs (from 28% to 81%) when compared with sham animals (72%–84%). Cardiac function was also assessed by CINE MRI at 22 weeks after surgery to allow a more in-depth analysis of the structural and functional remodeling in these animals. EFs measured after MI using CINE MRI and echocardiography at 22 weeks were tightly correlated and validated the use of echo at each time point (Figure IA in the Data Supplement). The use of echo was necessary to reduce the length of time the animals were under anesthesia because echo provides a quick, but reliable measurement of cardiac function.[22] EF at 1 and 22 weeks significantly correlated, indicating that cardiac function did not alter over the time of the experiment (Figure IB in the Data Supplement). Scar size, measured as the thinned and akinetic regions of the myocardium, negatively correlated with EF (determined using CINE MRI), ranging from 4% to 37% of the LV (Figure 1). End-diastolic volume also negatively correlated with EF, whereas cardiac output and stroke volume correlated positively with EF. The dilation of the LV and decrease in cardiac output were consistent with functional abnormalities associated with the progression into heart

failure. Average viable mass was not significantly different over the range of EFs, consistent with compensated hypertrophy of the remote myocardium (Figure II in the Data Supplement).

Altered In Vivo Metabolism in the Infarcted Heart

Hyperpolarized ^{13}C-MRS was used to measure the real-time conversion of [1-^{13}C]pyruvate into both [^{13}C]bicarbonate and $^{13}CO_2$, which directly assesses flux through PDH. At 1 and 6 weeks after induction of MI, there was no significant correlation between EF and PDH flux (Figure 2), despite several animals with severely reduced EFs. This result was supported by the group analysis, which revealed no significant difference between hearts with normal and impaired function (Figure III in the Data Supplement). This would imply that the contribution to energy generation from pyruvate was unaltered 6 weeks after infarction, despite observed functional deficits early after MI. However, by 22 weeks after surgery, a significant positive correlation between EF and PDH flux was observed (Figure 2; Figure III in the Data Supplement). Therefore by 22 weeks, the use of pyruvate for acetyl-CoA generation, and subsequent acetyl-CoA processing via the Krebs cycle, was reduced in infarcted hearts proportional to the degree of functional impairment. Incorporation of the hyperpolarized ^{13}C label into [1-^{13}C]lactate and [1-^{13}C]alanine was also evaluated in these experiments. No correlation between EF and ^{13}C-label incorporation from [1-^{13}C]pyruvate into [1-^{13}C]lactate was observed at any time point. At 1 and 22 weeks, ^{13}C-label incorporation into [1-^{13}C]alanine did not correlate with EF, interestingly although at 6 weeks, there was a significant positive correlation with EF. It is possible that these data indicate limited nonoxidative fates of pyruvate after MI surgery (Figure IV in the Data Supplement).

Altered In Vivo Activity of the Krebs Cycle

To evaluate the effects of MI on Krebs cycle metabolism, the conversion of [2-^{13}C]pyruvate into several downstream mitochondrial products, namely [5-^{13}C]glutamate, [1-^{13}C]citrate, and [1-^{13}C]acetylcarnitine, was also evaluated. Figure 3 shows a representative [2-^{13}C]pyruvate spectra from the 22-week time point of both a sham and an infarcted heart. ^{13}C-label incorporation into glutamate, citrate, and acetylcarnitine showed no significant correlation with EF at 1 week after surgery (Figure 4). However, at 6 weeks after MI, incorporation of the ^{13}C-label into the Krebs cycle (citrate) was reduced in proportion to contractile dysfunction, independent of any changes in PDH flux. This was also accompanied by a positive correlation between EF and ^{13}C-label flux into acetylcarnitine and glutamate. These findings were supported by the group analysis, which showed significant reductions in the levels of ^{13}C incorporation into citrate, glutamate, and acetylcarnitine in the hearts with impaired function (Figure V in the Data Supplement). Such results may reflect several different perturbations in these hearts, namely a reduction in the activity of the enzymes required to synthesize these products, or reductions in the pool sizes of these metabolites, or a combination of both. These changes in the Krebs cycle remained at 22 weeks after MI but were also accompanied by alterations in PDH flux. Therefore, the observed differences at this later time point were accompanied by decreased amounts of ^{13}C-label reaching the Krebs cycle because of decreased PDH flux.[20]

Altered In Vivo Metabolite Signals Over the Duration of the Study

A 2-way repeated measures ANOVA of the data revealed a general trend (statistically significant for all metabolites except lactate, data not shown) for ^{13}C-label incorporation to increase during the 22-week time frame of the study. This effect was caused by the ratiometric nature of the kinetic analysis that explored the relative proportion of metabolite generated from the injected ^{13}C-labeled pyruvate. As the amount of pyruvate injected was held constant across the time course of the study and the amount of viable myocardium in the sensitive region of the radiofrequency coil increased as the animals grew, an increase in the relative metabolite levels was observed.

Altered Metabolite Pool Sizes in the Infarcted Heart

In vitro ^{1}H-NMR spectroscopy was used to determine whether the decreased ^{13}C-label incorporation into the Krebs cycle was linked with alterations in the metabolite pool sizes at 22 weeks. The relative pool size of citrate did not significantly correlate with EF, thereby demonstrating that any reduction in the production of citrate must have also been coupled with a reduced use. In contrast to this, a positive correlation was observed between the pool sizes of both glutamate and malate, and EF, indicating depletion of Krebs cycle intermediates (Figure 5; Figure VI in the Data Supplement). Consistent with other studies of contractile dysfunction,[27–29] a positive correlation was seen between creatine and EF. Decreased creatine highlights an alteration in energy handling within the infarcted heart.

Alterations in Carnitine Availability in the Infarcted Heart

Carnitine is the carrier for mitochondrial membrane transport of fatty acyl-CoA and acetyl-CoA and exists as a finite pool within the heart. Direct infusion mass spectrometry was used to measure carnitine levels within the heart. Changes in carnitine availability could lead to alterations in acetylcarnitine production and, therefore, ^{13}C-label incorporation into [1-^{13}C] acetylcarnitine. There was a significant negative correlation between the ratio of acylcarnitine:free carnitine and cardiac function (Figure 5; Figure VII in the Data Supplement). Furthermore, the ratio of free carnitine:total carnitine positively correlated with cardiac function. Taken together, these findings suggest that there was a reduction in the relative availability of free carnitine in the infarcted hearts, which may make some contribution to the reduction in [1-^{13}C]acetylcarnitine.

MI Affected the Activity of Krebs Cycle Enzymes

Finally, to understand the observed alterations in in vivo flux through PDH and in the Krebs cycle, changes in key mitochondrial enzyme activities were assessed. Consistent with decreased flux into bicarbonate and CO_2, PDH activity positively correlated with EF at 22 weeks (Figure 6; Figure VIII in the Data Supplement).

The positive correlation of ^{13}C-label flux into acetylcarnitine and EF seems to have been driven by multiple factors. Along with altered carnitine availability, the activity of carnitine acetyl-transferase positively correlated with cardiac function, indicating that decreased ^{13}C-label incorporation might be a result of both decreased enzyme activity and decreased free carnitine. Decreased CS activity was also seen to correlate with cardiac function, demonstrating that altered ^{13}C-label flux into citrate was because of changes in CS activity

and not increased usage of citrate. Interestingly, aconitase activity did not significantly correlate with EF, suggesting that this enzyme reaction was not a rate-determining step, whereas isocitrate dehydrogenase (ICDH) activity was found to correlate with EF positively. Changes to both CS and ICDH activity mean that flux into glutamate, whether derived from the [2-^{13}C]pyruvate or endogenous substrates, will have been reduced. This would explain the observed reductions in both ^{13}C-label incorporation and glutamate pool size, which were proportional to cardiac function.

Discussion

An increasing body of evidence links alterations in cardiac metabolism with the progression of heart disease.[1] In this study, using hyperpolarized ^{13}C-MRS, an in vivo assessment of mitochondrial metabolism after MI was performed. At 6 weeks after MI, activity in the Krebs cycle positively correlated with cardiac function, indicative of early in vivo mitochondrial defects. Early metabolic alterations in the heart after MI occurred independently of changes in PDH flux, which were not observed until 22 weeks after MI.

Reduced Capacity to Oxidize Acetyl-CoA After MI

One week after MI, there were no detectable alterations in cardiac mitochondrial metabolism over the range of EFs observed. This was an early adaptive phase after infarction, where scar formation and remodeling of the heart were occurring.[30–32]

Six weeks after an MI, impairment in in vivo mitochondrial Krebs cycle activity was seen to correlate with the degree of cardiac dysfunction. Although the observation of mitochondrial Krebs cycle alteration after an MI is not novel, the fact that these were detected in vivo provides an interesting opportunity to monitor the effects of modified cardiac function on cardiac metabolism. Interestingly, these changes in Krebs cycle activity were independent of alterations in PDH. Thus, in vivo alterations in Krebs cycle activity may define an early maladaptive phase in metabolic derangement that is associated with the progression into heart failure. Reductions in ^{13}C-label incorporation into citrate and acetylcarnitine, which correlated with cardiac function, have highlighted a reduced capacity of the infarcted heart to oxidize acetyl-CoA, despite a normal ability to decarboxylate pyruvate. Uncoupling means acetyl-CoA is produced at the same rate by PDH, but there is a reduction in its oxidation because of a slowdown in Krebs cycle activity. Without information of β-oxidation, it is unclear whether changes in fatty acid usage lead to less acetyl-CoA from fat, thereby preventing the normal feedback inhibition of PDH.[33] Although altered ^{13}C-label incorporation into glutamate may have been a result of reduced label flux through CS, the reduced ^{13}C-label incorporation into citrate shows that in vivo the initial reactions of the Krebs cycle were defective at this early time point.

The animals were subsequently studied at 22 weeks after MI. CINE MRI analysis showed that, consistent with a 22-week chronically infarcted heart, EF positively correlated with scar size, indicating that LV remodeling was related to the degree of myocardial damage.[22] Measurements of the viable myocardium (both in vitro and in vivo using MRI) indicated no relationship between viable myocardium and EF at 22 weeks (Figure II in the Data Supplement), meaning that any decreases in in vivo ^{13}C-label incorporation were not

because of reductions in the mass of viable tissue in the infarcted hearts. At 22 weeks after MI, there was a general breakdown in in vivo mitochondrial function. Although EF remained relatively stable during the course of the study, the deterioration in in vivo mitochondrial function was progressive during the 22-week time frame. Along with the defects in Krebs cycle activity described at 6 weeks after MI, flux through PDH also correlated with cardiac function at the 22-week time point. These alterations highlight defects in pyruvate oxidation at 22 weeks after MI. Our in vivo data support and advance the link between cardiac and mitochondrial function, which has previously been reported in vitro.[5,6,8,34,35]

[13]C-label incorporation into citrate demonstrates the flux of pyruvate-derived acetyl-CoA into the Krebs cycle and provides a measure of Krebs cycle activity. Decreased ^{13}C-label incorporation into citrate at 22 weeks was because of multiple factors, including decreased CS activity and reduced acetyl-CoA production (by PDH). In vitro analysis of CS activity suggests that with more severe impairment of cardiac function, the enzyme becomes less efficient at producing citrate. Decreases in CS activity are widely reported after MI,[5,6,8,36,37] but the use of hyperpolarized ^{13}C-MRS has provided the first in vivo measurements of this occurring, which was recently highlighted as an important factor in understanding the development of heart failure.[38] Interestingly, ^{13}C-label incorporation into citrate did not relate to citrate pool size in this study because the pool size of citrate did not alter during the range of EFs observed. The maintenance of a normal citrate pool size was because of the decreased activity of ICDH, which along with CS, showed a positive correlation with EF.

Label incorporation into glutamate provided information on the activity of the initial reactions of the Krebs cycle. At both 6 and 22 weeks, positive correlations between cardiac function and ^{13}C-label incorporation into glutamate were observed, which were accompanied by a decreased glutamate pool size. The alteration in ICDH activity suggests a decrease in the production of α-ketoglutarate, which may explain both the decreased pool size and the reduced ^{13}C-label incorporation into glutamate. However, it does not preclude a possible contribution from increased α-ketoglutarate efflux in the reduction of ^{13}C incorporation into glutamate.[39,40] The reduction in myocardial glutamate levels, in addition to reduced malate levels, may also indicate alterations in the malate–aspartate shuttle.[41] In an environment where there is a reduced activity of both CS and ICDH, it is also possible that an increased mitochondrial uptake of glutamate may maintain α-ketoglutarate levels and keep the second span of the Krebs cycle flowing.[42]

At both 6 and 22 weeks, there was a reduced capacity for acetylcarnitine formation, which normally acts as a buffering system for excess acetyl-CoA production, similar to triacylglycerol in β-oxidation.[14] Reductions in ^{13}C-label flux into acetylcarnitine may be a indicative of a reduction in available free carnitine and reduced carnitine acetyl-transferase enzyme activity.[43,44] Previous data suggest that carnitine becomes trapped in the acylcarnitine form because of reductions in β-oxidation, therefore, preventing free carnitine from being available to buffer excess acetyl-CoA.[43,45–47] We have presented evidence here that this could be the case with a possible reduction in free carnitine in the viable myocardium of low EF animals at 22 weeks. Coupled with this, measurement of the activity of carnitine acetyl-transferase revealed that although reductions in free carnitine may play

some role in the reduced acetylcarnitine flux, the enzyme must also carry a defect, which reduces the activity. The breakdown of this auxiliary pathway could explain the reason for carnitine trapping, because of a reduction in free CoA, which is itself trapped in acetyl-CoA. This complicated cycle of trapping of CoA and carnitine eventually leads to reductions in PDH and Krebs cycle activity, and possibly β-oxidation, although this was not measured here.[48]

Limitations

As with any study, the limitations of the technique used need to be taken into consideration when interpreting the results. With the use of hyperpolarized pyruvate, there is a requirement for injection of supraphysiological concentrations of the tracer; however, the physiological effect of the pyruvate injection has previously been shown to be minimal.[16] In this study, sequential injections of hyperpolarized pyruvate (labeled at either the C1 or C2 positions) were given with an interval of 1 hour between injections. Although the order of the injections was randomized to ensure that there was no bias in the acquired data, there is the possibility that any long-term physiological effects of the multiple injections may have contributed to the level of variation observed in the acquired data.

Another limitation is that pyruvate only probes one side of the metabolic process, namely carbohydrate metabolism, and is unable to report directly on fatty acid oxidation. Recent advances in the field of hyperpolarized ^{13}C-MRS have allowed the use of butyrate as a metabolic probe for short-chain fatty acid metabolism. The use of this compound may provide more information on fatty acid metabolism in the infarcted heart.[49]

Although in previous studies using hyperpolarized pyruvate it has been possible to observe increases in the level of anaplerosis through the production of [3-^{13}C]citrate, it was not possible to quantify this peak in this study reliably.[23] This does not, however, rule out an increased reliance on anaplerosis in the infarcted heart, which has been observed previously in the diseased rat heart.[50]

Finally, the use of imaging of the metabolism of the infarcted heart would significantly strengthen this study. Although technical developments have been made to enable the imaging of hyperpolarized [1-^{13}C]pyruvate in the isolated rat heart, the ability to perform these studies has not yet been routinely translated into the in vivo rat heart.[51]

Conclusions

In this study, the ability of hyperpolarized 13C-MRS to measure in vivo alterations in cellular metabolism at multiple time points has offered new insights into the pathogenesis of heart failure after MI. The technique has shown that there were early maladaptive alterations to in vivo mitochondrial function at 6 weeks after MI, where Krebs cycle activity was reduced, whereas flux through PDH remained normal, possibly indicating an uncoupling of pyruvate oxidation and Krebs cycle activity. At 22 weeks, there were significant decreases in both PDH flux and label incorporation into the Krebs cycle, proportional to the decreased cardiac function. This may imply that alterations in the myocardial energy demand associated with diminished cardiac function lead to progressive alterations in Krebs cycle and PDH activity.

With the completion of the first human trials of hyperpolarized ^{13}C-MRS in cancer human applications for the study of in vivo cardiovascular metabolism is on the horizon.[52] The results from this study provide an interesting insight into the development of in vivo metabolic defects in the in vivo rat heart. With the continued development of this technology,[53] it is hoped that hyperpolarized ^{13}C-MRS will provide a useful diagnostic and prognostic tool in the study of the metabolic alterations in the ischemic and failing human heart.

Supplementary Material

Refer to Web version on PubMed Central for supplementary material.

Acknowledgments

References

1. Neubauer S. The failing heart—an engine out of fuel. N Engl J Med. 2007; 356:1140–1151. [PubMed: 17360992]

2. Opie, LH. Heart Physiology: From Cell to Circulation. 4th ed.. Lippincott Williams & Wilkins; Philadelphia: 2004.

3. Stanley WC, Recchia FA, Lopaschuk GD. Myocardial substrate metabolism in the normal and failing heart. Physiol Rev. 2005; 85:1093–1129. [PubMed: 15987803]

4. Lopaschuk GD, Ussher JR, Folmes CD, Jaswal JS, Stanley WC. Myocardial fatty acid metabolism in health and disease. Physiol Rev. 2010; 90:207–258. [PubMed: 20086077]

5. Heather LC, Cole MA, Lygate CA, Evans RD, Stuckey DJ, Murray AJ, Neubauer S, Clarke K. Fatty acid transporter levels and palmitate oxidation rate correlate with ejection fraction in the infarcted rat heart. Cardiovasc Res. 2006; 72:430–437. [PubMed: 17034771]

6. Heather LC, Catchpole AF, Stuckey DJ, Cole MA, Carr CA, Clarke K. Isoproterenol induces *in vivo* functional and metabolic abnormalities: similar to those found in the infarcted rat heart. J Physiol Pharmacol. 2009; 60:31–39. [PubMed: 19826179]

7. Stanley WC, Lopaschuk GD, Hall JL, McCormack JG. Regulation of myocardial carbohydrate metabolism under normal and ischaemic conditions. Potential for pharmacological interventions. Cardiovasc Res. 1997; 33:243–257. [PubMed: 9074687]

8. Heather LC, Carr CA, Stuckey DJ, Pope S, Morten KJ, Carter EE, Edwards LM, Clarke K. Critical role of complex III in the early metabolic changes following myocardial infarction. Cardiovasc Res. 2010; 85:127–136. [PubMed: 19666902]

9. Scheubel RJ, Tostlebe M, Simm A, Rohrbach S, Prondzinsky R, Gellerich FN, Silber RE, Holtz J. Dysfunction of mitochondrial respiratory chain complex I in human failing myocardium is not due to disturbed mitochondrial gene expression. J Am Coll Cardiol. 2002; 40:2174–2181. [PubMed: 12505231]

10. Ide T, Tsutsui H, Kinugawa S, Utsumi H, Kang D, Hattori N, Uchida K, Arimura Ki, Egashira K, Takeshita A. Mitochondrial electron transport complex I is a potential source of oxygen free radicals in the failing myocardium. Circ Res. 1999; 85:357–363. [PubMed: 10455064]

11. Lesnefsky EJ, Moghaddas S, Tandler B, Kerner J, Hoppel CL. Mitochondrial dysfunction in cardiac disease: ischemia–reperfusion, aging, and heart failure. J Mol Cell Cardiol. 2001; 33:1065–1089. [PubMed: 11444914]

12. Sivakumar R, Anandh Babu PV, Shyamaladevi CS. Protective effect of aspartate and glutamate on cardiac mitochondrial function during myocardial infarction in experimental rats. Chem Biol Interact. 2008; 176:227–233. [PubMed: 18786522]

13. Ardenkjaer-Larsen JH, Fridlund B, Gram A, Hansson G, Hansson L, Lerche MH, Servin R, Thaning M, Golman K. Increase in signal-to-noise ratio of > 10,000 times in liquid-state NMR. Proc Natl Acad Sci U S A. 2003; 100:10158–10163. [PubMed: 12930897]

14. Schroeder MA, Atherton HJ, Dodd MS, Lee P, Cochlin LE, Radda GK, Clarke K, Tyler DJ. The cycling of acetyl-coenzyme A through acetylcarnitine buffers cardiac substrate supply: a hyperpolarized 13C magnetic resonance study. Circ Cardiovasc Imaging. 2012; 5:201–209. [PubMed: 22238215]

15. Schroeder MA, Cochlin LE, Heather LC, Clarke K, Radda GK, Tyler DJ. *In vivo* assessment of pyruvate dehydrogenase flux in the heart using hyperpolarized carbon-13 magnetic resonance. Proc Natl Acad Sci U S A. 2008; 105:12051–12056. [PubMed: 18689683]

16. Atherton HJ, Schroeder MA, Dodd MS, Heather LC, Carter EE, Cochlin LE, Nagel S, Sibson NR, Radda GK, Clarke K, Tyler DJ. Validation of the *in vivo* assessment of pyruvate dehydrogenase activity using hyperpolarised 13C MRS. NMR Biomed. 2011; 24:201–208. [PubMed: 20799252]

17. Merritt ME, Harrison C, Storey C, Jeffrey FM, Sherry AD, Malloy CR. Hyperpolarized 13C allows a direct measure of flux through a single enzyme-catalyzed step by NMR. Proc Natl Acad Sci U S A. 2007; 104:19773–19777. [PubMed: 18056642]

18. Dodd MS, Ball V, Bray R, Ashrafian H, Watkins H, Clarke K, Tyler DJ. *In vivo* mouse cardiac hyperpolarized magnetic resonance spectroscopy. J Cardiovasc Magn Reson. 2013; 15:19. [PubMed: 23414451]

19. Golman K, Olsson LE, Axelsson O, Månsson S, Karlsson M, Petersson JS. Molecular imaging using hyperpolarized 13C. Br J Radiol. 2003; 76(Spec No 2):S118–S127. [PubMed: 15572334]

20. Dodd MS, Ball DR, Schroeder MA, Le Page LM, Atherton HJ, Heather LC, Seymour AM, Ashrafian H, Watkins H, Clarke K, Tyler DJ. *In vivo* alterations in cardiac metabolism and function in the spontaneously hypertensive rat heart. Cardiovasc Res. 2012; 95:69–76. [PubMed: 22593200]

21. Schroeder MA, Lau AZ, Chen AP, Gu Y, Nagendran J, Barry J, Hu X, Dyck JR, Tyler DJ, Clarke K, Connelly KA, Wright GA, Cunningham CH. Hyperpolarized (13)C magnetic resonance reveals early- and late-onset changes to *in vivo* pyruvate metabolism in the failing heart. Eur J Heart Fail. 2013; 15:130–140. [PubMed: 23258802]

22. Stuckey DJ, Carr CA, Tyler DJ, Clarke K. Cine-MRI versus two-dimensional echocardiography to measure *in vivo* left ventricular function in rat heart. NMR Biomed. 2008; 21:765–772. [PubMed: 18457349]

23. Atherton HJ, Dodd MS, Heather LC, Schroeder MA, Griffin JL, Radda GK, Clarke K, Tyler DJ. Role of pyruvate dehydrogenase inhibition in the development of hypertrophy in the hyperthyroid rat heart: a combined magnetic resonance imaging and hyperpolarized magnetic resonance spectroscopy study. Circulation. 2011; 123:2552–2561. [PubMed: 21606392]

24. Pearson, DJ.; Tubbs, PK.; Chase, FA. Carnitine and acylcarnitine. In: Bergmeyer, HU., editor. Methods of Enzymatic Analysis. Verlag Chemie, Academic Press; Weinheim, NY: 1974. p. 1758-1771.

25. Darley-Usmar, V.; Rickwood, D.; Wilson, M. Mitochondria, A Practical Approach. IRL Press; Oxford: 1987.

26. Atherton HJ, Gulston MK, Bailey NJ, Cheng KK, Zhang W, Clarke K, Griffin JL. Metabolomics of the interaction between PPAR-alpha and age in the PPAR-alpha-null mouse. Mol Syst Biol. 2009; 5:259. [PubMed: 19357638]

27. Zhang J, Merkle H, Hendrich K, Garwood M, From AH, Ugurbil K, Bache RJ. Bioenergetic abnormalities associated with severe left ventricular hypertrophy. J Clin Invest. 1993; 92:993–1003. [PubMed: 8349829]

28. Neubauer S, Horn M, Naumann A, Tian R, Hu K, Laser M, Friedrich J, Gaudron P, Schnackerz K, Ingwall JS. Impairment of energy metabolism in intact residual myocardium of rat hearts with chronic myocardial infarction. J Clin Invest. 1995; 95:1092–1100. [PubMed: 7883957]

29. Nascimben L, Ingwall JS, Pauletto P, Friedrich J, Gwathmey JK, Saks V, Pessina AC, Allen PD. Creatine kinase system in failing and nonfailing human myocardium. Circulation. 1996; 94:1894–1901. [PubMed: 8873665]

30. Ertl G, Frantz S. Healing after myocardial infarction. Cardiovasc Res. 2005; 66:22–32. [PubMed: 15769445]

31. Sun Y, Kiani MF, Postlethwaite AE, Weber KT. Infarct scar as living tissue. Basic Res Cardiol. 2002; 97:343–347. [PubMed: 12200633]

32. Zornoff LAM, Paiva SAR, Minicucci MF, Spadaro J. Experimental Myocardium Infarction in Rats: Analysis of the Model. Arq Bras Cardiol. 2008; 93:403–408.

33. Randle PJ, Garland PB, Hales CN, Newsholme EA. The glucose fatty-acid cycle. Its role in insulin sensitivity and the metabolic disturbances of diabetes mellitus. Lancet. 1963; 1:785–789. [PubMed: 13990765]

34. Sack MN, Rader TA, Park S, Bastin J, McCune SA, Kelly DP. Fatty acid oxidation enzyme gene expression is downregulated in the failing heart. Circulation. 1996; 94:2837–2842. [PubMed: 8941110]

35. Seymour AM, Chatham JC. The effects of hypertrophy and diabetes on cardiac pyruvate dehydrogenase activity. J Mol Cell Cardiol. 1997; 29:2771–2778. [PubMed: 9344771]

36. Lei B, Lionetti V, Young ME, Chandler MP, d'Agostino C, Kang E, Altarejos M, Matsuo K, Hintze TH, Stanley WC, Recchia FA. Paradoxical downregulation of the glucose oxidation pathway despite enhanced flux in severe heart failure. J Mol Cell Cardiol. 2004; 36:567–576. [PubMed: 15081316]

37. Razeghi P, Young ME, Alcorn JL, Moravec CS, Frazier OH, Taegtmeyer H. Metabolic gene expression in fetal and failing human heart. Circulation. 2001; 104:2923–2931. [PubMed: 11739307]

38. Westenbrink BD, Dorn GW II. Imaging the cardiac diet. Eur J Heart Fail. 2013; 15:123–124. [PubMed: 23329701]

39. Yu X, White LT, Doumen C, Damico LA, LaNoue KF, Alpert NM, Lewandowski ED. Kinetic analysis of dynamic 13C NMR spectra: metabolic flux, regulation, and compartmentation in hearts. Biophys J. 1995; 69:2090–2102. [PubMed: 8580353]

40. LaNoue K, Nicklas WJ, Williamson JR. Control of citric acid cycle activity in rat heart mitochondria. J Biol Chem. 1970; 245:102–111. [PubMed: 4312474]

41. LaNoue KF, Williamson JR. Interrelationships between malate-aspartate shuttle and citric acid cycle in rat heart mitochondria. Metabolism. 1971; 20:119–140. [PubMed: 4322086]

42. Sorokina N, O'Donnell JM, McKinney RD, Pound KM, Woldegiorgis G, LaNoue KF, Ballal K, Taegtmeyer H, Buttrick PM, Lewandowski ED. Recruitment of compensatory pathways to sustain oxidative flux with reduced carnitine palmitoyltransferase I activity characterizes inefficiency in energy metabolism in hypertrophied hearts. Circulation. 2007; 115:2033–2041. [PubMed: 17404155]

43. Suzuki Y, Masumura Y, Kobayashi A, Yamazaki N, Harada Y, Osawa M. Myocardial carnitine deficiency in chronic heart failure. Lancet. 1982; 1:116. [PubMed: 6119489]

44. Marquis NR, Fritz IB. The distribution of carnitine, acetylcarnitine, and carnitine acetyltransferase in rat tissues. J Biol Chem. 1965; 240:2193–2196. [PubMed: 14299646]

45. Calvani M, Reda E, Arrigoni-Martelli E. Regulation by carnitine of myocardial fatty acid and carbohydrate metabolism under normal and pathological conditions. Basic Res Cardiol. 2000; 95:75–83. [PubMed: 10826498]

46. Wittels B, Spann JF Jr. Defective lipid metabolism in the failing heart. J Clin Invest. 1968; 47:1787–1794. [PubMed: 4233124]

47. Rennison JH, McElfresh TA, Okere IC, Patel HV, Foster AB, Patel KK, Stoll MS, Minkler PE, Fujioka H, Hoit BD, Young ME, Hoppel CL, Chandler MP. Enhanced acyl-CoA dehydrogenase activity is associated with improved mitochondrial and contractile function in heart failure. Cardiovasc Res. 2008; 79:331–340. [PubMed: 18339649]

48. Abdel-aleem S, Nada MA, Sayed-Ahmed M, Hendrickson SC, St Louis J, Walthall HP, Lowe JE. Regulation of fatty acid oxidation by acetyl-CoA generated from glucose utilization in isolated myocytes. J Mol Cell Cardiol. 1996; 28:825–833. [PubMed: 8762022]

49. Ball DR, Rowlands B, Dodd MS, Le Page L, Ball V, Carr CA, Clarke K, Tyler DJ. Hyperpolarized butyrate: a metabolic probe of short chain fatty acid metabolism in the heart. Magn Reson Med. 2014; 71:1663–1669. [PubMed: 23798473]

50. Pound KM, Sorokina N, Ballal K, Berkich DA, Fasano M, Lanoue KF, Taegtmeyer H, O'Donnell JM, Lewandowski ED. Substrate-enzyme competition attenuates upregulated anaplerotic flux through malic enzyme in hypertrophied rat heart and restores triacylglyceride content: attenuating upregulated anaplerosis in hypertrophy. Circ Res. 2009; 104:805–812. [PubMed: 19213957]

51. Ball DR, Cruickshank R, Carr CA, Stuckey DJ, Lee P, Clarke K, Tyler DJ. Metabolic imaging of acute and chronic infarction in the perfused rat heart using hyperpolarised [1-13C]pyruvate. NMR Biomed. 2013; 26:1441–1450. [PubMed: 23775685]

52. Nelson SJ, Kurhanewicz J, Vigneron DB, Larson PE, Harzstark AL, Ferrone M, van Criekinge M, Chang JW, Bok R, Park I, Reed G, Carvajal L, Small EJ, Munster P, Weinberg VK, Ardenkjaer-Larsen JH, Chen AP, Hurd RE, Odegardstuen LI, Robb FJ, Tropp J, Murray JA. Metabolic imaging of patients with prostate cancer using hyperpolarized [1-^{13}C]pyruvate. Sci Transl Med. 2013; 5:198ra108.

53. Schroeder MA, Clarke K, Neubauer S, Tyler DJ. Hyperpolarized magnetic resonance: a novel technique for the *in vivo* assessment of cardiovascular disease. Circulation. 2011; 124:1580–1594. [PubMed: 21969318]

CLINICAL PERSPECTIVE

Hyperpolarized ^{13}C magnetic resonance spectroscopy provides an unprecedented sensitivity with which to study cardiac metabolism in real-time and in vivo. This article uses a rodent model of myocardial infarction to explore the links between functional and structural alterations in the heart after myocardial infarction and the resulting changes in cardiac metabolism. Six weeks after the induction of myocardial infarction, significant decreases in in vivo Krebs cycle flux were observed, which preceded alterations to pyruvate dehydrogenase flux, which were not observed until 22 weeks. These alterations may serve as valuable diagnostic markers for the decrease of glucose oxidation associated with the development into heart failure.
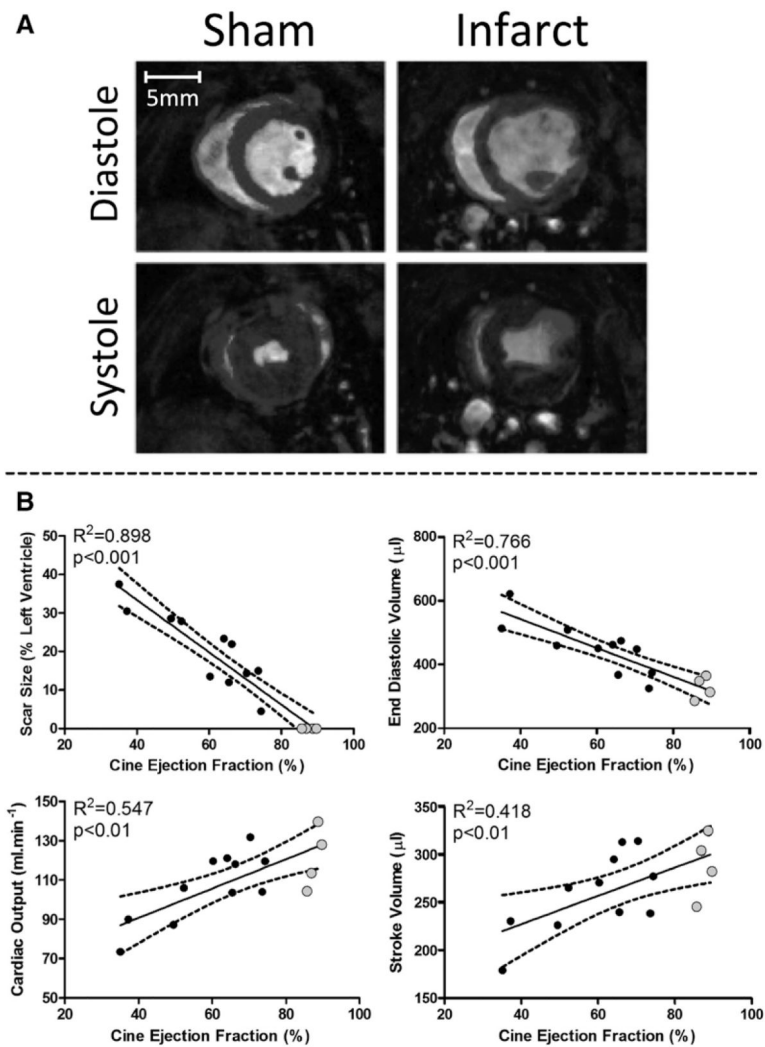
Figure 1.
Cardiac function. **A**, Example CINE MR images of a sham and infarcted heart at diastole and systole (**B**) CINE MR analysis at the 22-week time point. Ejection fraction significantly correlates with scar size, cardiac output, and stroke volume, which decrease, whereas end-diastolic volume increases. Gray dots highlight sham-operated animals.
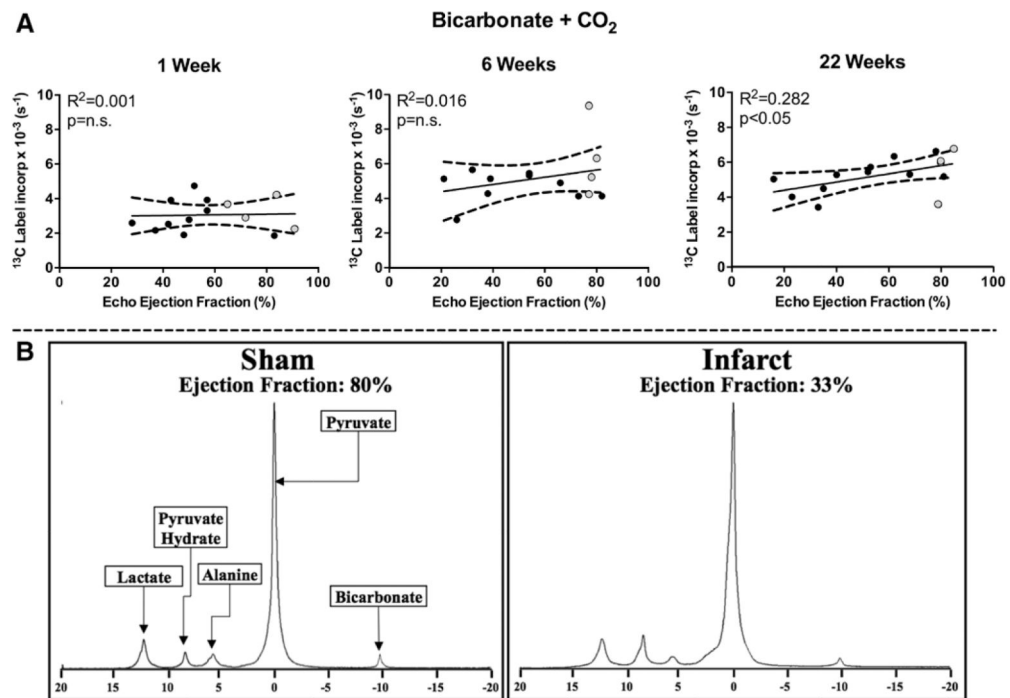
Figure 2.
In vivo flux through pyruvate dehydrogenase (PDH) was measured at 1, 6, and 22 weeks after myocardial infarction (MI). **A**, No change was seen in PDH flux (bicarbonate+CO_2) in the first 6 weeks after MI. By 22 weeks, PDH flux significantly correlated with ejection fraction (determined by echo). **B**, Representative 22-week spectra of [1-^{13}C]pyruvate metabolism in a sham and infarcted animal. In vivo ^{13}C label incorporation into bicarbonate was decreased in the infarcted heart when compared with sham heart. No change was seen for lactate or alanine. Pyruvate hydrate, the nonmetabolic product of pyruvate, is also shown. (week 6: bicarbonate+CO_2 was analyzed using Spearman Rank Correlation).
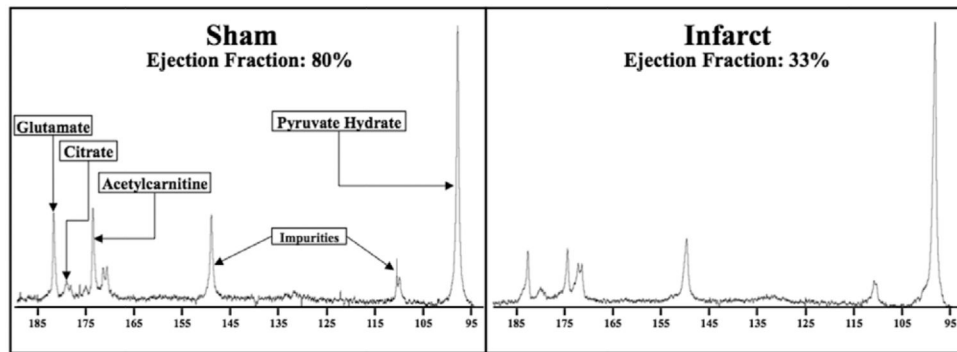
Figure 3.
Representative 22-week spectra of [2-^{13}C]pyruvate metabolism in a sham and infarcted animal: in vivo ^{13}C label incorporation into citrate, glutamate, and acetylcarnitine is decreased in the infarcted heart when compared with sham heart. This image is enlarged from the complete spectrum to highlight the glutamate, citrate, and acetylcarnitine peaks. Pyruvate hydrate, the nonmetabolic product of pyruvate, is used to provide scale.
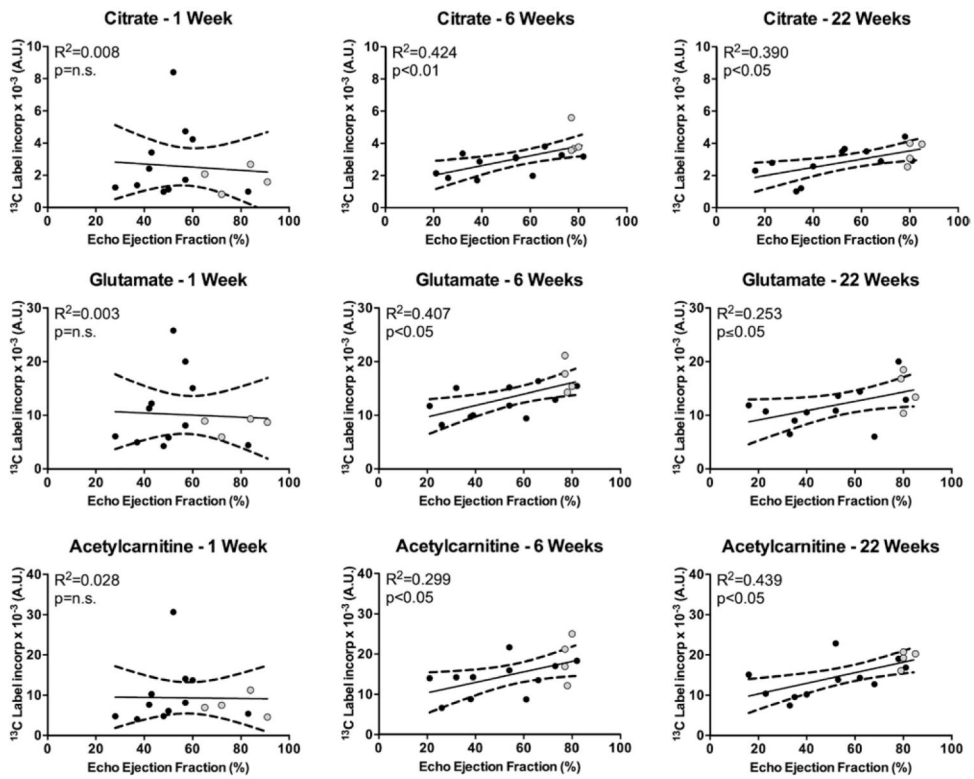
Figure 4.
In vivo ^{13}C label incorporation into citrate, glutamate, and acetylcarnitine 1, 6, and 22 weeks after myocardial infarction: at 6 and 22 weeks, ^{13}C label incorporation into the Krebs cycle and acetylcarnitine correlated with ejection fraction (week 1: acetylcarnitine was analyzed using Spearman Rank Correlation).
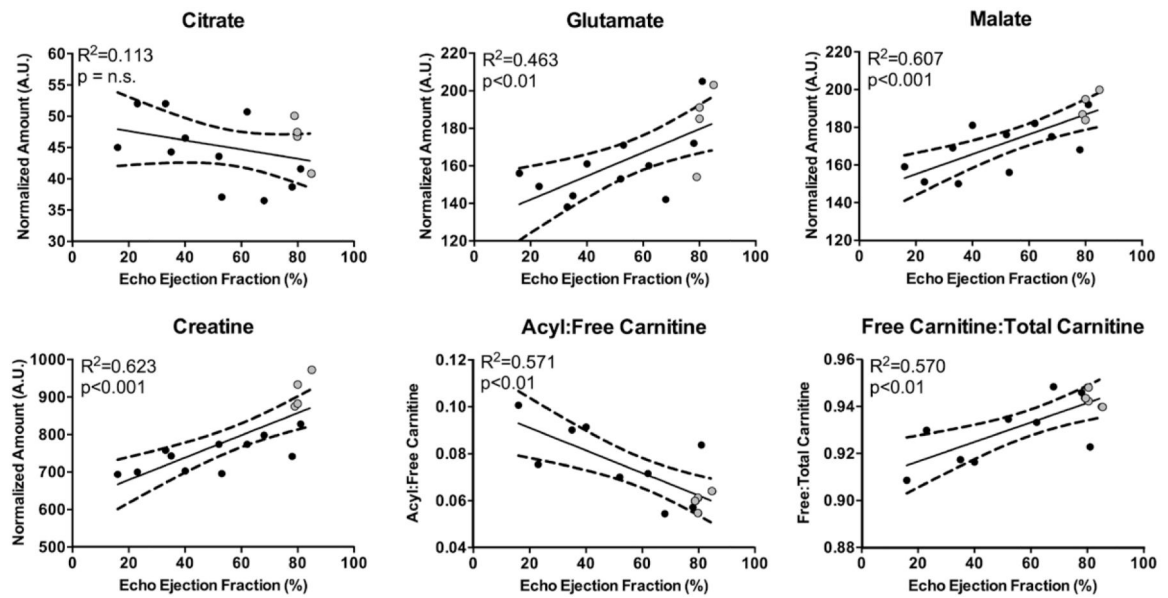
Figure 5.
In vitro metabolomic analysis of Krebs cycle intermediates and other relevant cellular metabolites showed alterations in the infarcted heart: at the 22-week time point, metabolic analysis showed that citrate levels were unaltered, whereas glutamate, malate, and creatine levels correlated positively with ejection fraction. The ratio of carnitine in the acylcarnitine to free carnitine negatively correlated with ejection fraction. This was driven by decreases in the free carnitine to total carnitine levels, which is indicative of carnitine deficiency.
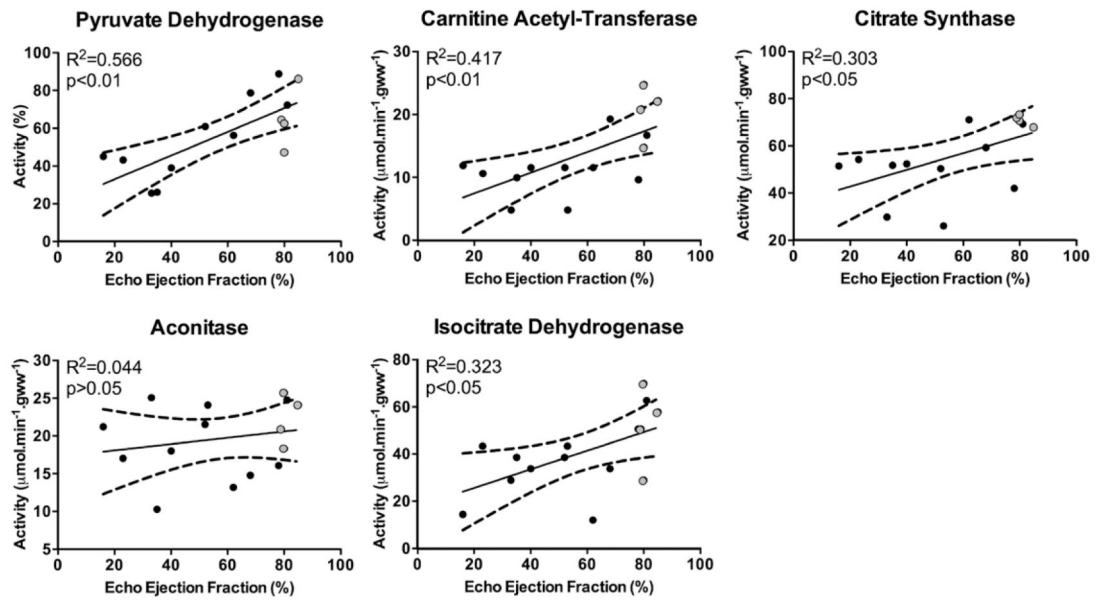
Figure 6.

In vitro analysis of key metabolic enzymes reveals reduced activity in the failing heart: consistent with in vivo data, pyruvate dehydrogenase, citrate synthase, and carnitine acetyl-transferase activity positively correlated with ejection fraction. Aconitase activity was unaltered with altered ejection fraction, possibly because this enzyme is not a rate-determining step. However, isocitrate dehydrogenase did show reduced activity with reduced cardiac function. Highlighting abnormalities in key enzymes involved in pyruvate oxidation and Krebs cycle flux with reducing ejection fraction.